ARTICLE

OBC
www.rsc.org/obc

Polymer-supported manganese porphyrin catalysts—peptide-linker promoted chemoselectivity

Emilie Brulé,[a] King Kuok (Mimi) Hii[b] and Yolanda R. de Miguel*[c]

[a] *Department of Chemistry, Organic Chemistry, Royal Institute of Technology, SE-10044, Stockholm, Sweden*

[b] *Department of Chemistry, Imperial College London, South Kensington, UK SW7 2AZ. E-mail: mimi.hii@imperial.ac.uk*

[c] *LABEIN Technological Centre, Calle Geldo, Edificio 700, Parque Tecnológico de Bizkaia, Derio, 48160, Bizkaia, Spain. E-mail: ydemiguel@labein.es; Fax: +34 94 607 3349*

Received 11th February 2005, Accepted 5th April 2005
First published as an Advance Article on the web 18th April 2005

Manganese porphyrin catalysts were tethered to polymer-supports *via* peptide linkers. The reactivity and chemoselectivity of the catalysts were assessed in the epoxidation of limonene. It was found that the inclusion of a peptide linker incorporating a donor heteroatom which could act as an axial ligand led to a supported manganese porphyrin catalyst with unprecedented selectivity and stability.

Introduction

The reactive site of many hemeproteins comprises a metalloporphyrin coordinated by a proximal ligand in the form of an amino acid residue in the protein scaffold, containing a sulfur, nitrogen or oxygen donor group in its side chain, *e.g.* cysteine, histidine or tyrosine residues are found in very different heme systems. A significant body of work has demonstrated that the proximal ligand controls the redox properties of the hemeproteins, thus determining the types of oxidation they can perform.[1] In the emerging area of protein engineering, there are also several reports on synthetic heme–peptide complexes with interesting catalytic, electrochemical and optical properties.[2–4]

There have been several recent reports of polymer-supported metalloporphyrins for the oxidation of olefins,[5] including our work on immobilised manganese porphyrin catalysts and their catalytic activity in the epoxidation of a wide range of alkenes[6a] and dienes.[6b] Many other studies on supported metalloporphyrins have also been published.[7–9] In our own studies we have highlighted distinct compatibility issues between the linker and the activity and recyclability of the supported catalysts. In particular, Wang-supported manganese porphyrins were found to display a fairly high regioselectivity in the epoxidation of limonene (2.7 : 1 in favour of the 1,2-regiomer). Reports by others[8] have also examined the chemoselective epoxidation of limonene using immobilised manganese porphyrins, as well as a zeolite-encapsulated ruthenium porphyrin. However, the chemoselectivities were no higher than 3 : 1 for previously reported supported manganese porphyrins.

Previously, the catalytic behaviour of a surface-bound manganese porphyrin–peptide conjugate in the oxidation of a number of alkenes was studied in the presence of iodosylbenzene.[9] It was found that incorporation of a peptide led to different yields and ratios of oxidised products, compared to control experiments conducted with the analogue without the peptide. More interestingly, substrate competition experiments showed that the catalyst was able to discriminate between alkenes of different sizes, demonstrating that the peptide chain was able to influence the reactivity of the metalloporphyrin. These results prompted us to speculate that peptide linkers may be able to promote the selectivity of polymer-bound mangenese porphyrins in alkene epoxidation reactions. Herein, the preparation of three polymer-supported manganese porphyrins containing different peptide linkers is described. These three different peptide linkers were chosen in order to test whether the different amino acid sequences were tolerated under the oxidation reaction conditions. Limonene is commonly used[10] to probe the steric hindrance of metalloporphyrins and was therefore chosen as the substrate for testing our new supported porphyrins. Their catalytic activity, chemoselectivity and recyclability were assessed with respect to the peptide chain length and constituent amino acid residues.

Results and discussion

Utilising solid-phase synthesis, Wang–Ala–Fmoc and Wang–Ile–Fmoc resins were functionalised with peptide linkers. Successive deprotection and coupling with Fmoc-protected amino acids were carried out using PyBOP–HOBt coupling reagents (Scheme 1). The yield of each step of the coupling was calculated by conducting the Fmoc test and the resultant functionalised polymers were fully characterised by a combination of % N analysis, single bead transmittance FTIR and gel-phase MAS–NMR spectroscopy. A library of more than 100 supported peptides was prepared in this way, but for the present study the synthesis of three representative supported peptides **1**–**3** is presented. They were chosen for their different spacer chain lengths as well as for their different peptide sequences containing amino acids with different functionalities (alkyl, N- or S-containing amino acids).

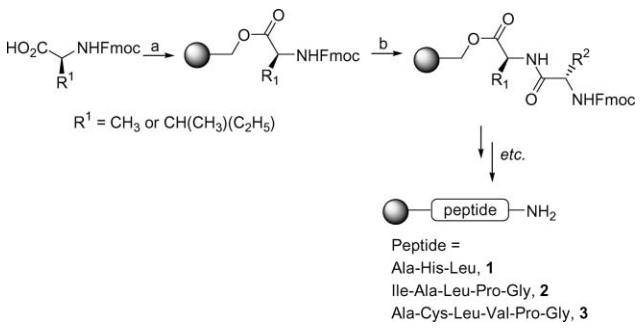

Scheme 1 Preparation of supported peptides: a) Wang resin, MSNT, MeIm, DCM, rt, 3 h; b) (i) 20% piperidine, DMF, rt, 15 min, (ii) Fmoc-protected amino acid, PyBOP, HOBt, DIPEA, DCM, DMF, rt, 3 h.

To maximise the interaction between the peptide chain and the metal centre, the porphyrin ring is attached to the peptide linker *via* the *ortho*-position of one of the peripheral phenyl

DOI:10.1039/b502149a

groups. Hence, 2-(10,15,20-triphenyl-porphyrin-5-yl)-phenol **4**[11] was initially subjected to an alkylation reaction with ethyl-4-bromobutyrate, then hydrolysed to give the functionalised porphyrin **6**. Subsequent treatment with $MnCl_2$ at reflux furnished the manganese(III) porphyrin complex **7** (Scheme 2). Finally, coupling of **7** with functionalised polymers **1–3** was achieved by using PyBOP–HOBt as coupling reagents, furnishing the corresponding manganese porphyrin–peptide conjugates WANG–Ala–His–Leu–*o*-MnP (**8**), WANG–Ile–Ala–Leu–Pro–Gly–*o*-MnP (**9**) and WANG–Ala–Cys–Leu–Val–Pro–Gly–*o*-MnP (**10**) (Fig. 1). ICP–AES analysis of these dark coloured beads showed the Mn loading percentage to be between 1.00–1.93 mmol g^{-1}.

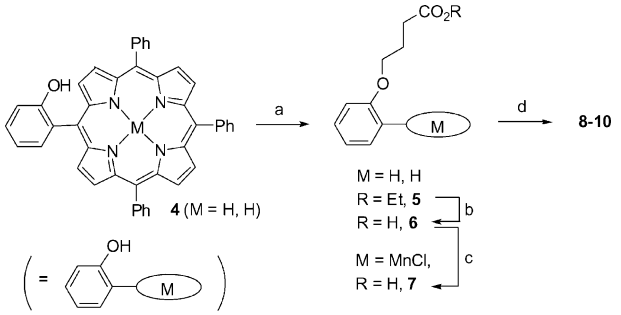

Scheme 2 Preparation of manganese porphyrins with a flexible tether: a) $BrCH_2CH_2CH_2CO_2Et$ (3.75 eq.), K_2CO_3, KI, dry DMF, 60 °C, 89%; b) (i) 1M aq. NaOH, THF, 48 h, rt, (ii) 10% w/w aq. AcOH; c) 20 eq. $MnCl_2$, dry DMF, 30 min, reflux; d) peptide **1**, **2** or **3**, PyBOP, HOBt, DIPEA, CH_2Cl_2, DMF, 3 h, rt.

The activity, selectivity and recyclability of these polymer-supported catalysts were subsequently examined in the epoxidation of limonene, which has been previously shown[10] to be sensitive to steric effects (Scheme 3). Using previously established catalytic assay conditions,[6b] the epoxidation of limonene proceeded smoothly, generating the 1,2-limonene oxide **11** as the major product. As a control experiment, it was checked that no product was formed in the presence of a Wang supported peptide without manganese porphyrin, nor with a metal-free porphyrin as a catalyst. It has also been previously demonstrated[6b] that Wang resin is stable during epoxidation reactions using sodium periodate as an oxidant.

Good chemoselectivity was obtained with all three catalysts **8–10** (Table 1). Most encouragingly, the tripeptide–manganese

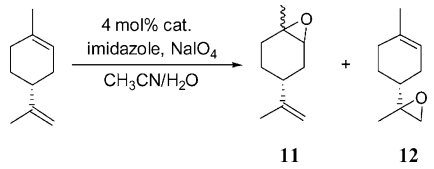

Scheme 3 Regioselective epoxidation of (*R*)-limonene.

porphyrin **8** displayed an excellent chemoselectivity of 5 : 1 (entry 3), which is the best reported so far for supported metalloporphyrin systems. The lowest ratio of 2.8 : 1 (entry 6), obtained with the pentapeptide–manganese porphyrin conjugate **9**, was comparable to that previously obtained with Wang supported catalysts without peptide linkers.[6] Catalyst **10**, with the longest peptide linker, appears to exhibit intermediate chemoselectivity (3.7 : 1, entry 9), but both yield and selectivity reached a plateau at 24 h. Notable also is the increase in chemoselectivity of catalyst **8**, which increases as the reaction progresses between 24 and 36 hours (entries 2 and 3). This is an interesting divergence from the steady chemoselectivity exhibited by the other two catalysts between 24 and 36 hours. This perhaps suggests the operation of competitive catalytic pathways with different selectivities in this particular system. In fact, it is also possible that a conformational change occurs as the reaction proceeds, leading to a more sterically-demanding catalyst structure and therefore to a higher chemoselectivity.

The relative rates of the catalytic turnovers were also monitored (Fig. 2). As expected, fast initial conversions were displayed by catalysts attached to longer peptide tethers, presumably due to greater catalyst mobility. However, there is marked difference in the stability of the catalysts after 12 h. Although catalyst **8** exhibited the slowest turnover it is the most stable, continuing to exhibit turnovers beyond 36 h, compared to catalysts **9** and **10**, which reached optimal conversions after 10 h. As the stability is clearly not dependent on the length of the peptide chain, we postulate that the robustness of catalyst **8** may be due to the presence of the *N*-donor group afforded by the histidine residue, which may act as a coordinating axial ligand and thus stabilise the reactive manganese metal centre (Fig. 3). The model also suggests that the epoxidation of the alkene will occur on the site opposite to the axial ligand and away from any chiral pocket that may be generated by the peptide chain. Hence, it is perhaps unsurprising that the reactions proceeded with no stereoselectivity, with de and ee values <3%.

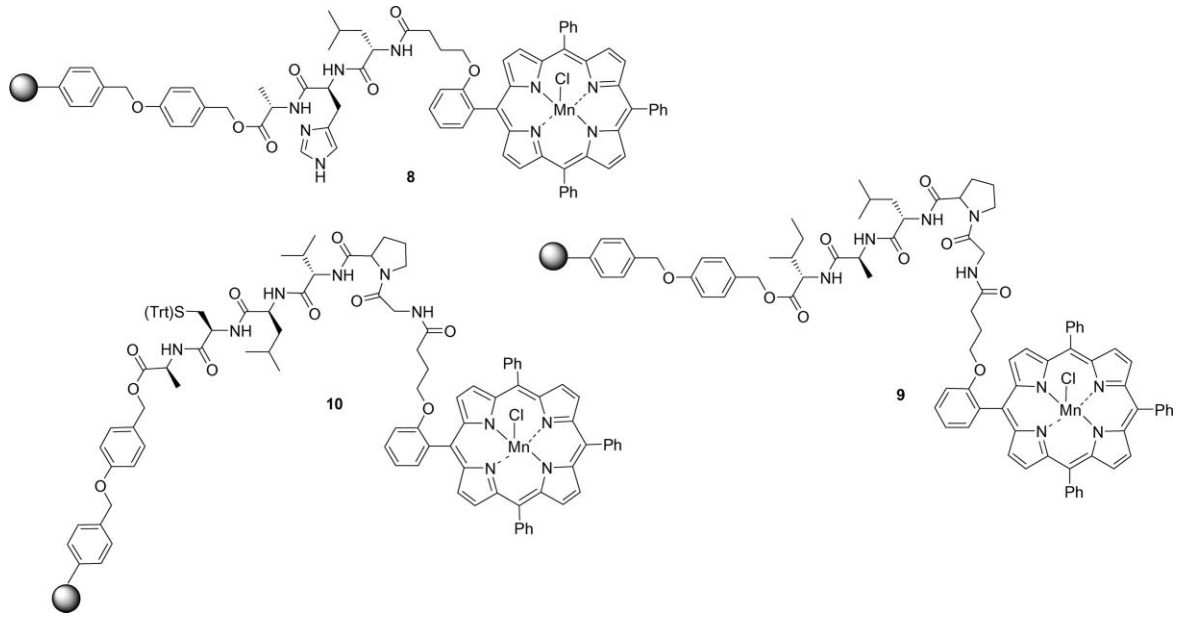

Fig. 1 Supported catalysts containing tri-, penta- and hexa-peptide linkers **8–10**.

Table 1 Regioselective epoxidation of (*R*)-limonene catalysed by immobilised peptide–manganese porphyrin conjugates **8–10**[a]

Entry	Catalyst	Time/h	Conversion[b] (%)	Yield[c] **11** (%)	Yield[c] **12** (%)	**11** : **12**
1	**8**	6	17	12	5	2.4 : 1
2		24	72	57	15	3.8 : 1
3		36	85	70	15	5 : 1
4	**9**	6	31	31	11	2.8 : 1
5		24	30	30	13	2.8 : 1
6		36	37	37	13	2.8 : 1
7	**10**	6	47	35	12	2.9 : 1
8		24	66	52	14	3.7 : 1
9		36	66	52	14	3.7 : 1

[a] Conditions: catalyst, imidazole, alkene, $NaIO_4$ in a molar ratio of 1 : 10 : 23 : 46, CH_3CN, H_2O (2 : 1). [b] Determined by GC analysis and corresponds to the percentage of starting material consumed. [c] GC yields with respect to starting material, yields were repeatable within ±2%.

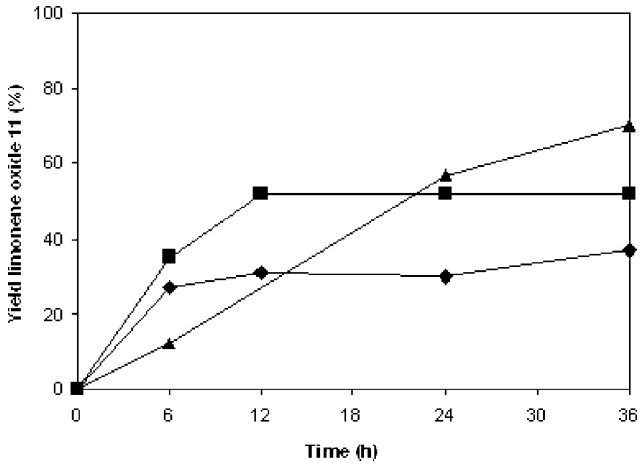

Fig. 2 Rates of reaction catalysed by **8** (triangles), **9** (diamonds) and **10** (squares).

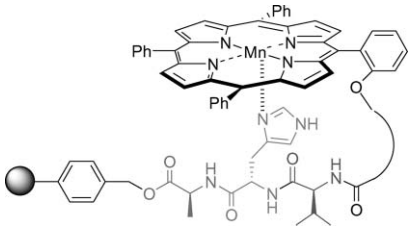

Fig. 3 Stabilisation of the catalyst **8** by the peptide linker.

Recyclability

The recovery and reuse of immobilised catalysts is often challenging since the catalyst may leach from the support or degrade under the oxidative conditions, resulting in the deactivation of the supported catalyst at the end of the first cycle and preventing further reuse. Previously reported recyclability studies of immobilised epoxidation catalysts were not always successful.[12]

Furthermore, claims on the recyclability of the supported catalysts "without significant loss of activity" were rarely backed up by experimental data and the chemoselectivity of the recycled catalysts was not discussed. In light of this, we examined the reuse of the immobilised peptide–manganese porphyrin conjugates **8**, **9** and **10** in the epoxidation of limonene.

UV spectroscopic examination of the catalytic reaction mixture showed the absence of any absorption peak due to free or manganese porphyrins, which served as the first indication that no leaching of the catalyst had occurred. This was confirmed by % Mn analysis of the recovered beads, which showed that there was no decrease of Mn content after recycling. The FT-IR spectra of the recovered catalysts were found to be identical to those of the freshly prepared samples.

Furthermore, the recovered polymer beads remained catalytically active in a second catalytic run (Fig. 4). With the tri- and hexapeptide supported catalysts **8** and **10**, similar conversions were obtained over 24 h, despite a slightly slower reactivity of the recycled catalyst during the initial 12 h. The chemoselectivity was also identical to that obtained in the first catalytic run (from the start of the reaction). In contrast, the pentapeptide supported catalyst **9** was far less active, achieving only half the conversion in the second catalytic run with a slight erosion in the chemoselectivity (2.5 : 1).

Conclusions

We have demonstrated that peptide linkers may be used as effective tethers for manganese porphyrins to polymer-supports. No catalyst leaching was observed and good chemoselectivity was obtained (5 : 1) with the tripeptide conjugate catalyst **8**. There seemed to be a correlation between the peptide chain length and the initial rates of reaction. However, the stability of these catalysts appears to be far less dependent on the chain length of the linker than on its constituent amino acid residues. For example, the presence of a coordinating side chain in the peptide linker of **8** (Fig. 3) is thought to lead to a stabilised and sterically-demanding catalyst structure. It exhibits good chemoselectivity as well as improved stability, which leads to retained catalytic activity in a second run. Other peptide

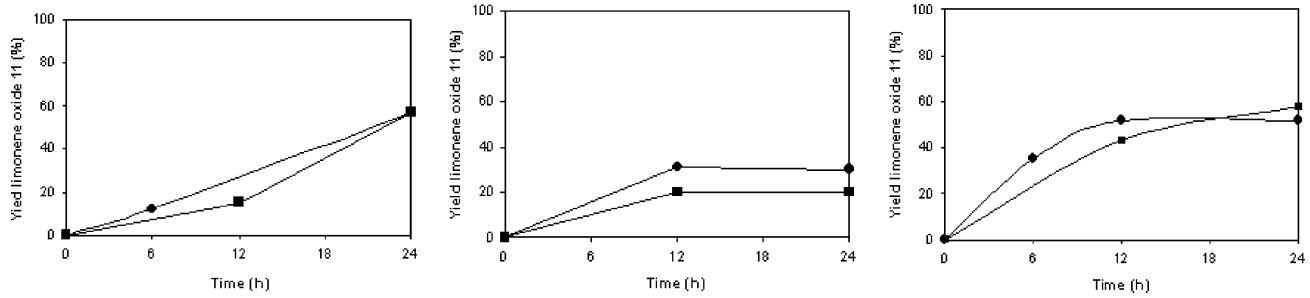

Fig. 4 Reaction progress for first (circle) and second (square) catalytic runs for catalysts **8** (left), **9** (middle) and **10** (right).

sequences in **9** and **10** gave poorer chemoselectivities, indicating that the conformational structure of the peptide–porphyrin catalyst is important. Future studies will focus on the systematic variation of the peptide structure in order to prepare and screen libraries of such olefin epoxidation catalysts.

Experimental

Materials

Wang–Ala–Fmoc (1.1 mmol g^{-1}) and WG–Ile–Fmoc (0.8 mmol g^{-1}) resins are 1% cross-linked with bead sizes between 100–200 mesh and were purchased from Novabiochem. Fmoc-protected peptides and the peptide coupling reagents (MSNT, HOBt and PyBOP) were also purchased from Novabiochem. Anhydrous DMF was bought from Aldrich and dichloromethane was freshly distilled from CaH_2 under nitrogen. $MnCl_2$ was purchased from Aldrich with 99.999% purity and supplied in ampoules, which were stored under nitrogen after opening.

Instrumental methods

The semi-automated peptide synthesiser is a Quest 210 (Argonaut Technologies) and contains twenty reactors with an internal volume of 5 mL. It is combined with an automated solvent wash unit. Single bead FT-IR spectra (transmittance) were recorded on a Perkin Elmer Spectrum One spectrometer with a beam-condensing accessory (BCA), using a diamond compressor to flatten the bead. Gel-phase high resolution magic angle spinning (HR-MAS) NMR spectra were recorded using a Bruker AVANCE 400 spectrometer with special HR-MAS probe and the resin was placed in a 4 mm rotor. GC-MS spectra were recorded on a Varian Saturn 220 spectrometer equipped with an autosampler. The carrier gas was helium and the flow rate was 1 mL min^{-1}. The chiral column used for the asymmetric epoxidation reactions was a cyclodex-B column, with an isothermal oven temperature of 100 °C. The Fmoc test was performed to determine the yield of peptide coupling reactions on the polymer-resin.

General procedure for the synthesis of deprotected supported peptides (manually or using the peptide semi-automated synthesiser)

The appropriate *N*-deprotected WG–peptide (0.1 mmol) was swollen in dry CH_2Cl_2 (10 mL) in a reaction flask under N_2. In another flask, the appropriate Fmoc-protected amino acid (0.5 mmol), PyBOP (0.26 g, 0.5 mmol) and HOBt (0.067 g, 0.5 mmol) were dissolved in dry DMF (10 mL) under N_2. Anhydrous DIPEA (0.17 mL, 1 mmol) was then added to the solution, which was stirred for a few minutes before it was added to the resin. The mixture was stirred at rt for 3 h. The resin was then filtered off and washed with acetone–CH_3OH (1 : 1) (3 mL × 5), acetone–CH_3OH–H_2O (1 : 1 : 1) (3 mL × 5), acetone–CH_3OH (1 : 1) (3 mL × 5), EtOAc (3 mL × 5), CH_2Cl_2 (3 mL × 5) and HPLC-grade pentane (3 mL × 5). The resin was dried in a vacuum oven for 3 h at 60 °C. Fmoc test or N-percentage analysis were used to determine the yield of attachment of the amino acid. The deprotection of the Fmoc group was performed by stirring the dried beads (0.36 g) in a solution of 20% piperidine in DMF (5 mL) for 15 min. The resin was then washed with CH_2Cl_2 and HPLC-grade pentane and dried in a vacuum oven for 3 h at 60 °C.

WG–Ala–His(Trt)–Leu 1.

WG–Ala–His(Trt). Yield: 95%, calculated from Fmoc test. ν_{max}/cm^{-1} 3377 (NH), 1718 $(C=O)_{ester}$, 1679 $(C=O)_{amide}$; δ_H (400 MHz, $CDCl_3$) 7.52 (br s, NH *Ala*), 4.97 (br s, NH_2 *His*), 4.60 (br s, H-α *Ala*), 3.67 (br s, H-α *His*), 2.99 (br s, H-β *His*), 1.35 (br s, H-β *Ala*).

WG–Ala–His(Trt)–Leu ***1***. Yield: 100%, calculated from Fmoc test. ν_{max}/cm^{-1} 3362br (NH), 1720 $(C=O)_{ester}$, 1676 $(C=O)_{amide}$; δ_H (400 MHz, $CDCl_3$) 8.45 (br s, NH *His*), 7.88 (br s, NH *Ala*), 4.95 (br s, NH_2 Leu)), 4.71 (br s, H-α *His*), 4.54 (br s, H-α *Ala*), 3.42 (br s, H-α *Leu*), 3.01 (br s, H-β *His*), 1.45 (br s, H-γ *Leu*), 1.35 (br s, H-β *Ala*, H-β *Leu*), 0.93 (br s, H-δ *Leu*).

WG–Ile–Ala–Leu–Pro–Gly 2.

WG–Ile–Ala. Yield: 100%, calculated from Fmoc test. ν_{max}/cm^{-1} 3375 (NH), 1739 $(C=O)_{ester}$, 1679 $(C=O)_{amide}$; δ_H (400 MHz, $CDCl_3$) 7.84 (br s, NH *Ile*), 4.96 (br s, NH_2 *Ala*), 4.62 (br s, H-α *Ile*), 3.53 (br s, H-α *Ala*), 1.96 (br s, H-β *Ile*), 1.42 (br s, H-γ *Ile*), 1.35 (br s, H-β *Ala*), 1.18 (br s, H′-γ *Ile*), 0.91 (br s, H-δ *Ile*).

WG–Ile–Ala–Leu. Yield: 93%, calculated from Fmoc test. ν_{max}/cm^{-1} 3329br (NH), 1738 $(C=O)_{ester}$, 1670br $(C=O)_{amide}$; δ_H (400 MHz, $CDCl_3$) 7.85 (br s, NH *Ile*, NH *Ala*), 4. 97 (br s, NH_2 *Leu*), 4.61 (br s, H-α *Ile*, H-α *Ala*), 3.40 (br s, H-α *Leu*), 1.95 (br s, H-β *Ile*), 1.74 (br s, H-β *Leu*), 1.40 (br s, H-β *Ala*, H-γ *Ile*, H-γ *Leu*), 1.19 (br s, H′-γ *Ile*), 0.98–0.95 (br s, H-δ *Ile*, H-δ Leu).

WG–Ile–Ala–Leu–Pro. Yield: 94%, calculated from Fmoc test. ν_{max}/cm^{-1} 3322br (NH), 1738 $(C=O)_{ester}$, 1671br $(C=O)_{amide}$.

WG–Ile–Ala–Leu–Pro–Gly ***2***. Yield: 90%, calculated from Fmoc test. ν_{max}/cm^{-1} 3313br (NH), 1736 $(C=O)_{ester}$, 1670br $(C=O)_{amide}$.

WG–Ala–Cys(Trt)–Leu–Val–Pro–Gly 3.

WG–Ala–Cys(Trt). Yield: 100%, calculated from Fmoc test. ν_{max}/cm^{-1} 3382 (NH), 1721 $(C=O)_{ester}$, 1681 $(C=O)_{amide}$; δ_H (400 MHz, $CDCl_3$) 8.08 (br s, NH *Ala*), 4.96 (br s, NH_2 *Cys*), 4.53 (br s, H-α *Ala*), 3.26 (br s, H-α *Cys*), 2.60 (br s, H-β *Cys*), 1.35 (br s, H-β *Ala*).

WG–Ala–Cys(Trt)–Leu. Yield: 100%, calculated from Fmoc test. ν_{max}/cm^{-1} 3363br (NH), 1739 $(C=O)_{ester}$, 1672 $(C=O)_{amide}$; δ_H (400 MHz, $CDCl_3$) 7.82 (br s, NH *Ala*), 7.66 (br s, NH *Cys*), 4.85 (br s, NH_2 *Leu*), 4.59 (br s, H-α *Ala*), 4.06 (br s, H-α *Cys*), 3.36 (br s, H-α *Leu*), 2.60 (br s, H-β *Cys*), 1.69 (br s, H-γ *Leu*), 1.49 (br s, H-β *Leu*), 1.35 (br s, H-β *Ala*), 0.94 (br s, H-δ *Leu*).

WG–Ala–Cys(Trt)–Leu–Val. Yield: 100%, calculated from Fmoc test. ν_{max}/cm^{-1} 3331br (NH), 1738 $(C=O)_{ester}$, 1674 $(C=O)_{amide}$; δ_H (400 MHz, $CDCl_3$) 7.74 (br s, NH *Ala*, NH *Cys*, NH *Leu*), 4.96 (br s, NH_2 *Val*), 4.60 (br s, H-α *Ala*), 4.43 (br s, H-α *Cys*), 3.75 (br s, H-α *Leu*), 3.18 (br s, H-α *Val*), 2.65 (br s, H-β *Cys*), 2.29 (br s, H-β *Val*), 1.67 (br s, H-γ *Leu*), 1.46 (br s, H-β *Leu*), 1.35 (br s, H-β *Ala*), 0.97 (br s, H-δ *Val*), 0.92 (br s, H-δ *Val*, H-δ *Leu*).

WG–Ala–Cys(Trt)–Leu–Val–Pro. Yield: 100%, calculated from Fmoc test. ν_{max}/cm^{-1} 3330br (NH), 1740 $(C=O)_{ester}$, 1673br $(C=O)_{amide}$.

WG–Ala–Cys(Trt)–Leu–Val–Pro–Gly ***3***. Yield: 100%, calculated from Fmoc test. ν_{max}/cm^{-1} 3313br (NH), 1740 $(C=O)_{ester}$, 1673br $(C=O)_{amide}$; δ_H (400 MHz, $CDCl_3$) 7.47 (br s, NH *Ala*, NH *Cys*, NH *Leu*, NH *Val*), 4.94 (br s, NH_2 *Gly*), 4.65 (br s, H-α *Leu*), 4.52 (br s, H-α *Ala*, H-α *Cys*, H-α *Val*, H-α *Pro*), 3.75 (br s, H-α *Gly*), 3.45 (br s, H-δ *Pro*), 2.65 (br s, H-β *Cys*), 2.21 (br s, H-β *Val*, H-β *Pro*), 1.59 (br s, H-γ *Leu*, H-γ *Pro*), 1.46 (br s, H-β *Leu*), 1.35 (br s, H-β *Ala*), 0.92 (br s, H-δ *Val*, H-δ *Leu*).

4-[2-(10,15,20-Triphenyl-porphyrin-5-yl)-phenoxy]-butyric acid ethyl ester 5. A mixture of 2-(10,15,20-triphenyl-porphyrin-5-yl)-phenol **4** (0.1 g, 0.16 mmol), ethyl-4-bromobutyrate (74 μl, 0.52 mmol), anhydrous K_2CO_3 (0.1 g, 0.74 mmol) and a catalytic amount of KI (50 mg, 0.3 mmol) was stirred in dry DMF (5 mL) under N_2 for 20 h at 60 °C. The mixture was then poured into 24 mL of a H_2O–CH_3OH solution (5 : 1). The purple precipitate formed was filtered and washed with a H_2O–CH_3OH solution. The solid was purified by column chromatography (silica gel, $CHCl_3$–hexane 8 : 2). The first fraction corresponded to the desired porphyrin ester as a purple solid and the second

fraction contained unreacted 2-(10,15,20-triphenyl-porphyrin-5-yl)-phenol **4**. Yield: 0.1 g, (0.14 mmol, 89%). R_f = 0.59 ($CHCl_3$–hexane 8 :2); mp >220 °C; $\lambda_{max}(CH_2Cl_2)$/nm 419 (ε/L $mol^{-1}cm^{-1}$ 185 029), 514 (8089), 549 (2652), 589 (1893), 646 (1492); $\nu_{max}(CCl_4$ solution)/cm^{-1} 3319 (NH), 1734 (C=O); δ_H (360 MHz, $CDCl_3$) 8.86–8.82 (8H, m, H_7, H_8), 8.28–8.20 (6H, m, $H_{2'}$–Ph), 8.06 (1H, dd, *J* 7.3 and 1.6, H_6–Ar), 7.80–7.71 (10H, m, $H_{4'}$–Ph, $H_{3'}$–Ph, H_4–Ar), 7.38 (1H, t, *J* 7.3 Hz, H_5–Ar), 7.34 (1H, d, *J* 7.4, H_3–Ar), 3.96 (2H, s br, OCH_2CH_2), 3.63 (2H, q, *J* 7.1, OCH_2CH_3), 1.34 (4H, s br, CH_2CO, $CH_2CH_2CH_2$), 0.78 (3H, t, *J* 7.1, CH_3), −2.72 (2H, s, NH); δ_C (90.5 MHz, $CDCl_3$) 173.2 (C=O), 159.0 (C_2–Ar), 142.7 ($C_{1'}$–Ph, C_1–Ar), 136.1 (C_6–Ar), 135.0 ($C_{2'}$–Ph), 133.0–131.0 (multiple broadened and weak signals C_7, C_8), 130.3 (C_4–Ar), 128.0 ($C_{4'}$–Ph), 127.0 ($C_{3'}$–Ph), 120.6 (C_{10}), 120.4 (C_5), 120.1 (C_5–Ar), 116.7 (C_3–Ar), 67.5 (OCH_2CH_2), 61.1 (OCH_2CH_3), 23.0 (CH_2CO), 24.2 ($CH_2CH_2CH_2$), 14.2 (CH_3); *m*/*z* (ES) 745 ([MH]$^+$, 92%), 279 (8), 147 (15), 100 (28), 64 (100); HRMS (ES): exact mass calcd for $C_{50}H_{40}N_4O_3$: 745.3173, found: 745.3185.

4-[2-(10,15,20-Triphenyl-porphyrin-5-yl)-phenoxy]-butyric acid 6. A solution of aqueous NaOH (60 mL, 1 M) was added to a solution of 4-[2-(10,15,20-triphenyl-porphyrin-5-yl)-phenoxy]-butyric acid ethyl ester **2** (0.15 g, 0.2 mmol) in THF (50 mL) at rt. The mixture was stirred for 2 days at rt. A solution of acetic acid–H_2O (1 : 9) (*ca.* 50 mL) was then added to the reaction mixture until pH = 7 was reached (pH paper). The reaction mixture was then extracted with chloroform (3 × 50 mL). The organic extracts were washed with a saturated $NaHCO_3$ solution (2 × 30 mL), H_2O (2 × 30 mL), dried ($MgSO_4$), filtered and evaporated to yield a purple solid. A minimum amount of CH_3OH was added to the flask containing the solid, which was filtered off and washed with a small amount of CH_3OH. The purple solid was then dried under a vacuum. Yield: 0.12 g, (0.16 mmol, 82%); mp >220 °C; $\lambda_{max}(CH_2Cl_2)$/nm 418 (ε/L $mol^{-1}cm^{-1}$ 153 078), 515 (8647), 550 (3088), 590 (2229), 646 (1719); $\nu_{max}(CCl_4$ solution)/cm^{-1} 3313 (NH), 2956 (OH), 1717 (C=O); δ_H (360 MHz, $CDCl_3$–CD_3OD 3 : 1) 8.75–8.70 (8H, m, H_7, H_8), 8.15–8.08 (6H, m, $H_{2'}$–Ph), 7.98 (1H, dd, *J* 7.3 and 1.6, H_6–Ar), 7.68–7.64 (10H, m, $H_{4'}$–Ph, $H_{3'}$–Ph, H_4–Ar), 7.29 (1H, t, *J* 7.3, H_5–Ar), 7.20 (1H, m, H_3–Ar), 3.83 (2H, t, *J* 5.3, OCH_2CH_2), 1.18–1.15 (4H, m, CH_2CO, $CH_2CH_2CH_2$); δ_C (90.5 MHz, $CDCl_3$–CD_3OD 3 : 1) 177.8 (C=O), 158.9 (C_2–Ar), 142.6 ($C_{1'}$–Ph, C_1–Ar), 136.0 (C_6–Ar), 135.9 ($C_{2'}$–Ph), 133.0–131.0 (multiple broadened and weak signals C_7, C_8), 130.3 (C_4–Ar, $C_{4'}$–Ph), 127.0 ($C_{3'}$–Ph), 120.5 (C_{10}), 120.4 (C_5), 120.1 (C_5–Ar), 116.5 (C_3–Ar), 67.3 (OCH_2CH_2), 29.5 (CH_2CO), 23.9 ($CH_2CH_2CH_2$); *m*/*z* (ES) 717 ([MH]$^+$, 100%), 142 (13), 121 (10), 149 (12), 64 (100); HRMS (ES): exact mass calcd for $C_{48}H_{37}N_4O_3$: 717.2860, found: 717.2860.

Manganese(III) chloride 4-[2-(10,15,20-triphenyl-porphyrin-5-yl)-phenoxy]-butyric acid 7. 4-[2-(10,15,20-Triphenyl-porphyrin-5-yl)-phenoxy]-butyric acid **6** (0.15 g, 0.2 mmol) was dissolved in anhydrous DMF (20 mL) under N_2. The purple solution was heated at reflux for 10 min before the addition of solid $MnCl_2$ (0.5 g, 4 mmol). The purple solution became green after a few min and the progress of the reaction was monitored by the disappearance of the UV absorption peak at 420 nm. At the end of the reaction (about 30 min), the reaction mixture was cooled in an ice bath and cold water (30 mL) was added until a green precipitate appeared. The solid was filtered off, washed with H_2O and dried under a vacuum to yield the manganese porphyrin. Yield: 0.13 g, (0.158 mmol, 79%); mp >220 °C; $\lambda_{max}(CH_2Cl_2)$/nm 345 (ε/L $mol^{-1}cm^{-1}$ 13 731), 380 (17 828), 402 (16 017), 478 (28 594), 580 (3056), 615 (2651); $\nu_{max}(CHCl_3$ solution)/cm^{-1} 2928 (OH), 1735 (C=O); *m*/*z* (ES) 769 ([M − $^{35}Cl]^+$, 100%), 136 (4), 95 (8), 74 (27), 64 (43); HRMS (ES): exact mass calcd for $C_{48}H_{34}N_4O_3Mn$: 769.2006, found: 769.1999.

General procedure for the synthesis of supported peptide-metalloporphyrin conjugates

The appropriate deprotected Wang supported peptide (1 mmol) was swollen in dry CH_2Cl_2 (20 mL) under N_2. In a separate flask under N_2, manganese(III) chloride 4-[2-(10,15,20-triphenyl-porphyrin-5-yl)-phenoxy]-butyric acid **7** (3 mmol), PyBOP (0.78 g, 3 mmol) and HOBt (0.2 g, 3 mmol) were dissolved in anhydrous DMF (20 mL) under N_2. Anhydrous DIPEA (0.52 mL, 6 mmol) was then added to this solution, which was stirred for a few minutes before addition to the resin. The mixture was then stirred at rt for 3 h. The resin was filtered and washed with acetone (3 mL × 5), acetone–H_2O (1 : 1) (3 mL × 5), acetone (3 mL × 5), EtOAc (3 mL × 5), CH_2Cl_2 (3 mL × 5) and HPLC-grade pentane (3 mL × 5). The resin was dried in a vacuum oven for 3 h at 60 °C.

WG–Ala–Cys–(Trt)–Leu–*o*-MnP 8. Yield: 100%, Mn 1.00%. ν_{max}/cm^{-1} 3396 (NH), 1720 $(C=O)_{ester}$, 1675 $(C=O)_{amide}$.

WG–Ile–Ala–Leu–Pro–Gly–*o*-MnP 9. Yield: 88%, Mn 1.53%. ν_{max}/cm^{-1} 3324br (NH), 1740 $(C=O)_{ester}$, 1665br $(C=O)_{amide}$.

WG–Ala–Cys(Trt)–Leu–Val–Pro–Gly–*o*-MPn 10. Yield: 100%, Mn 1.93%. ν_{max}/cm^{-1} 3388br (NH), 1721 $(C=O)_{ester}$, 1662br $(C=O)_{amide}$.

General procedure for epoxidation

In a round-bottomed flask or in a Radley's carousel reaction tube, the appropriate catalyst (0.01 mmol), alkene (0.23 mmol) and axial ligand (0.1 mmol) were stirred in CH_3CN (3.7 mL) at rt. In a separate flask, $NaIO_4$ (0.46 mmol) was dissolved in H_2O (1.85 mL). This aq. solution of $NaIO_4$ was added to the catalytic mixture. The progress of the reaction was monitored by taking aliquots of the solution at regular intervals *via* syringe and they were analysed by GC-MS. The yields of epoxides were based on the starting material and the precentage conversion corresponds to the starting material consumed.

Test for catalyst leaching

In order to determine if catalyst leaching occurred, the solution of the epoxidation reaction was extracted with CH_2Cl_2, washed with water, dried over Na_2SO_4 and evaporated. A small amount of the residue obtained was dissolved in dichloromethane and analysed by UV spectroscopy. In case of leaching, a peak corresponding to manganese(III) porphyrin would be visible at $\lambda = 480$ nm.

General procedure for the recovery and reuse of the catalyst

At the end of the epoxidation, the polymer-supported catalyst was collected *via* a filter syringe. The catalyst beads in the syringe were washed with water, CH_2Cl_2 and HPLC-grade pentane and then dried under a vacuum at 50 °C for 2 h. The recovered catalyst was then used for a second cycle of the epoxidation reaction as described above.

Acknowledgements

The authors thank King's College London for studentship support (to E. B.) and The Royal Society for a Dorothy Hodgkin Fellowship (to Y. d. M.) and for an Instrumentation Grant for the procurement of the QUEST210 reaction station.

References

1 (*a*) L. J. Marnett and T. A. Kennedy, in *Cytochrome P450: Structure, Mechanism and Biochemistry*, ed. P. R. Ortiz de Montellano, Plenum Press, New York, 1995, pp. 49–80; (*b*) J. P. Collman, R. Boulatov, C. J. Sunderland and L. Fu, *Chem. Rev.*, 2004, **104**, 561–588; (*c*) C. J. Reedy and B. R. Gibney, *Chem. Rev.*, 2004, **104**, 617–649; (*d*) B. Meunier, S. P. de Visser and S. Shaik, *Chem. Rev.*, 2004, **104**, 3947–3980.

2 D. L. Huffman, M. M. Rosenblatt and K. S. J. Suslick, *J. Am. Chem. Soc.*, 1998, **120**, 6183–6184.
3 H. K. Privett, C. J. Reedy, M. L. Kennedy and B. R. Gibney, *J. Am. Chem. Soc.*, 2002, **124**, 6828–6829.
4 J. J. Mao, K. Hauser and M. R. Gunner, *Biochemistry*, 2003, **42**, 9829–9840.
5 (*a*) C. Du, Z. Li, X. Wen, J. Wu, X. Yu, M. Yang and R. Xie, *J. Mol. Catal. A: Chem.*, 2004, **216**, 7–12; (*b*) M. Moghadam, S. Tangestaninejad, M. H. Habibi and V Mirkhani, *J. Mol. Catal. A: Chem.*, 2004, **217**, 9–12 and references therein.
6 (*a*) E. Brulé and Y. R. de Miguel, *Tetrahedron Lett.*, 2002, **43**, 8555–8558; (*b*) E. Brulé, Y. R. de Miguel and K. K. Hii, *Tetrahedron*, 2004, **60**, 5913–5918.
7 (*a*) Smith J. R. Lindsay, in *Metalloporphyrins in Catalytic Oxidations*, ed. R. A. Sheldon, Marcel DekkerNew York, 1994, pp. 350–368 and references therein; (*b*) M. Benaglia, T. Danelli and G. Pozzi, *Org. Biomol. Chem.*, 2003, **1**, 454–456.
8 (*a*) C.-J. Liu, W.-Y Yu., S.-G. Li and C.-M. Che, *J. Org. Chem.*, 1998, **63**, 7364–7369; (*b*) V. Mirkhani, S. Tangestaninejad and M. Moghadam, *J. Chem. Res., Synop.*, 1999, 722–723; (*c*) S. Tangestaninejad and M. Moghadam, *J. Chem. Res., Synop.*, 1998, 242–243; (*d*) S. Tangestaninejad and M. Moghadam, *Synth. Commun.*, 1998, **28**, 427–432; (*e*) S. Tangestaninejad, M. H. Habib, V. Mirkhani and M. Moghadam, *J. Chem. Res., Synop.*, 2001, 444–445; (*f*) S. Tangestaninejad and V. Mirkhani, *J. Chem. Res.*, 1998, 788–789; (*g*) S. Tangestaninejad, M. H. Habibi, V. Mirkhani and M. Moghadam, *Synth. Commun.*, 2002, **32**, 3331–3337.
9 (*a*) G. R. Geier and T. Sasaki, *Tetrahedron*, 1999, **55**, 1859–1870; (*b*) G. R. Geier and T. Sasaki, *Tetrahedron Lett.*, 1997, **38**, 3821–3824.
10 D. Mansuy, J. F. Bartoli, P. Battioni, D. K. Lyon and R. G. Finke, *J. Am. Chem. Soc.*, 1991, **113**, 7222–7226.
11 F. d'Souza, S. Gadde, M. E. Zandler, K. Arkady, M. E. El-Khouly, M. Fujitsuka and O. Ito, *J. Phys. Chem. A*, 2002, **106**, 12393–12404.
12 For example, see: (*a*) M. D. Angelino and P. E. Laibinis, *J. Polym. Sci., A: Polym. Chem.*, 1999, **37**, 3888–3898; (*b*) L. Canali, E. Cowan, H. Deleuze, C. L. Gibson and D. C. Sherrington, *J. Chem. Soc., Perkin Trans. 1*, 2000, 2055–2066.